

# Generation of sea-level curves from depositional pattern as seen through seismic attributes-seismic geomorphology analysis of an MTC-rich shallow sediment column, northern Gulf of Mexico

SUPRATIK SARKAR, KURT J. MARFURT, and ROGER M. SLATT, *University of Oklahoma*

Detailed interpretation of seismic attributes along horizon slices or stratal slices reveals changes in depositional pattern and seismic geomorphology within a sediment column that are controlled by eustatic and local changes in sea level. In this study, we analyze seismic geomorphologic features of a shallow sedimentary column within a salt minibasin in the northern Gulf of Mexico, and attempt to predict the relative sea-level curves. We then calibrate these predictions against biostratigraphic markers and compare with existing eustatic cycles and events. Systematic analysis of amplitude and attribute data within a seismic geomorphologic framework reveals high-resolution sequence stratigraphic patterns that might otherwise be overlooked.

## Introduction

Our study area is within the tabular salt minibasin tectono-stratigraphic province (Diegel et al., 1995) of the northern Gulf of Mexico (GOM) margin (Figure 1a). Salt constrains the minibasin on the eastern, western, and southern sides; the main sediment fairway is from the northeastern side (Figure 1b). Due to the constrained sediment fairway, limited accommodation space, and deposition by “fill and spill” processes (e.g., Winker, 1996), the geomorphology of deep-water deposits within salt minibasins differs from that in unconfined marine conditions.

Deepwater clastic deposits consist of four main architectural or depositional elements: channels, thin-bed levees,

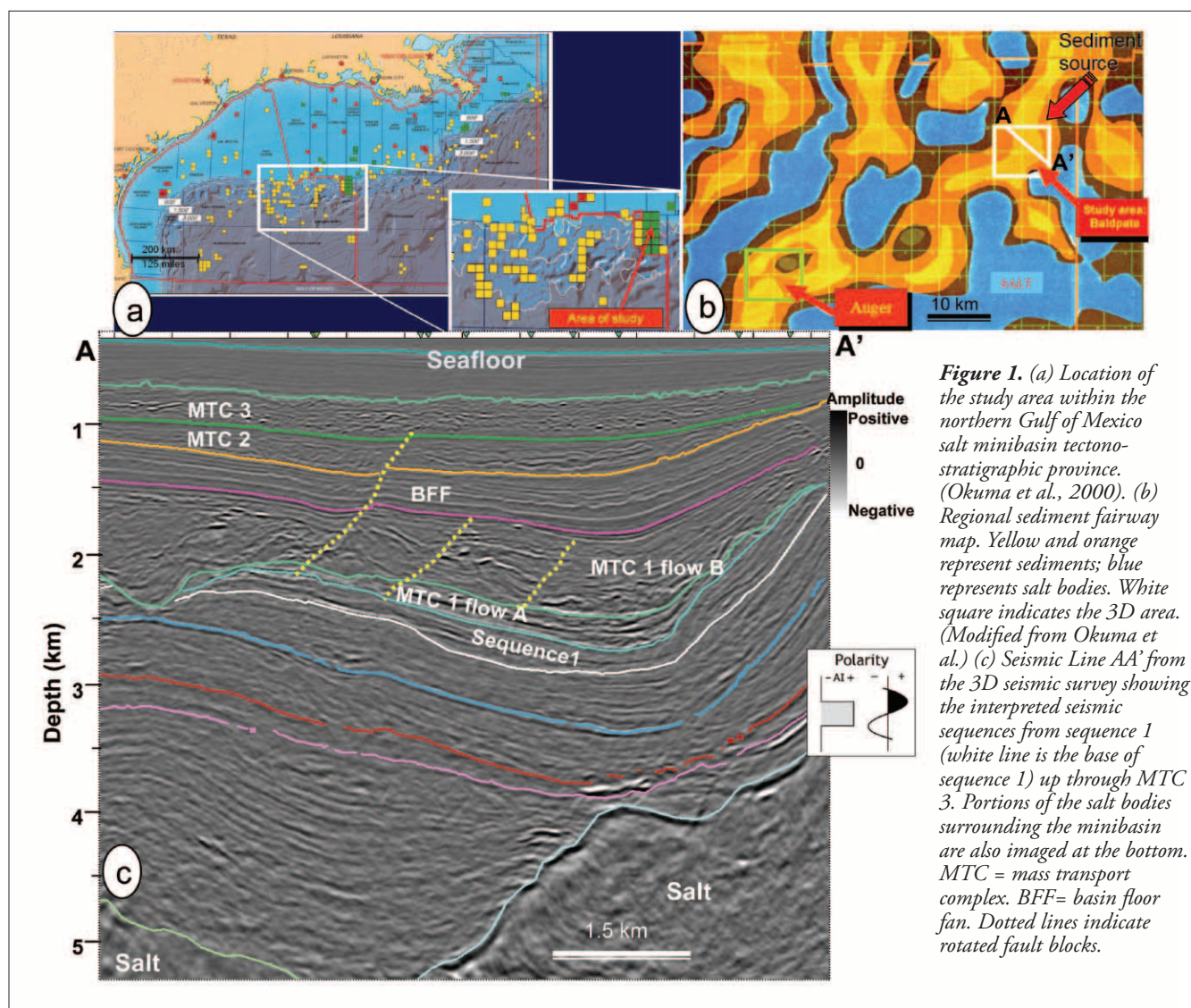


**Figure 1.** (a) Location of the study area within the northern Gulf of Mexico salt minibasin tectono-stratigraphic province. (Okuma et al., 2000). (b) Regional sediment fairway map. Yellow and orange represent sediments; blue represents salt bodies. White square indicates the 3D area. (Modified from Okuma et al.) (c) Seismic Line AA' from the 3D seismic survey showing the interpreted seismic sequences from sequence 1 (white line is the base of sequence 1) up through MTC 3. Portions of the salt bodies surrounding the minibasin are also imaged at the bottom. MTC = mass transport complex. BFF = basin floor fan. Dotted lines indicate rotated fault blocks.



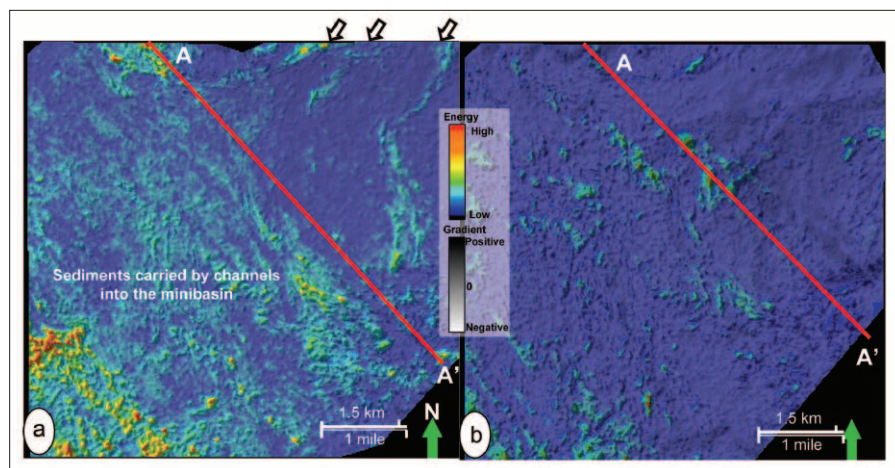


**Figure 2.** Phantom horizon slices blending coherent energy and inline gradient attributes approximately (a) 250 m below and (b) 125 m below the top of sequence 1 (Figure 1c), computed using a three-trace by three-trace by five-sample analysis window ( $75 \times 75 \times 45$  m). In (a) arrows indicate a channel system coming from the northeast and (b) exhibits an overall low-amplitude character.

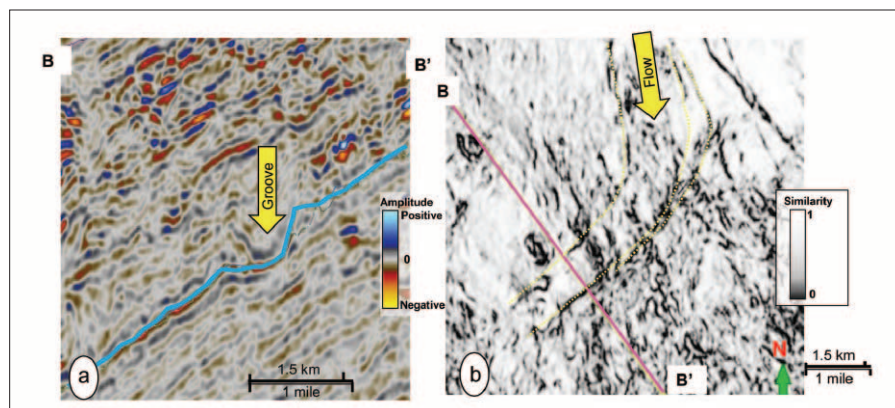


**Figure 3.** Striation or groove seen in (a) vertical seismic indicated by yellow arrow and (b) horizon slice along the cyan pick on (a) through the generalized Sobel filter similarity volume. Dotted yellow lines in (b) indicate the edges of the groove while the arrow indicates the flow direction.

basin floor fans or sheets, and mass transport complexes (MTC). The shallow sediment column we are studying here is dominated by MTCs along with other architectural elements. MTCs generally form due to slope failure or slumping from the shelf-slope area when sea level falls rapidly, exposing the shelf-slope area and changing sediment pore pressure. Sediment accumulation in the system of salt minibasins takes place in a “fill and spill” process (e.g., Winker, 1996) from upslope to downslope areas, thereby preserving the basin floor fan and channel-levee sediments related with the basin processes. While traditionally MTCs go from upslope to downslope from shelf to slope regions, in areas of salt tectonism MTCs can also have a local origin due to slope failure or enhanced salt diapirism. Mass transport complexes can be subdivided into (1) slide, (2) slump, and (3) debrites, or any combination of the three. Where slide and slump are related to sliding and slumping of deposited sediments, debrites are high-density flows in which coarser particles are supported by matrix strength. Although there are examples of reservoir

units from each type of MTC, these are rare in nature. In general, mass transport complexes exhibit a chaotic seismic reflection pattern. This chaotic pattern differentiates MTCs from more layered fans, channel sands and pelagic shales.

In this study, we analyzed a 100-km<sup>2</sup> prestack depth-migrated 3D seismic volume that covers almost the entire minibasin (Figure 2). Well logs and sparse biostratigraphic data constrain our seismic interpretation. We identify three MTC units (denoted as MTC 1, 2, and 3) as well as seismic sequences containing sheet sands, and channels (Figure 2).

In addition to the migrated seismic amplitude, we generated a suite of seismic attribute volumes including rms amplitude, coherent energy (the square of the rms amplitude of the coherent component of the data), energy ratio similarity, generalized Sobel filter edge detectors, amplitude gradients, and spectral decomposition components. Although attributes such as rms amplitude, coherence, and curvature are mathematically independent, they are often coupled through the underlying geology. For this reason, some features can be identified on all attributes while others were illuminated by only one or two attributes.

### Sequential seismic geomorphologic analysis

**MTC 1 and underlying sequence 1.** We start with “sequence 1” underlying MTC 1 (Figure 1c), where attribute expressions indicate the presence of a channel system (Figure 2a). In Figure 2b, we display the phantom horizon slice through blended coherent energy and inline amplitude gradient volumes, approximately 125 m below the top of sequence 1. The low-amplitude deposits in Figure 2b indicate fine-grained sediments throughout the minibasin.

We identify a few striations or grooves at the base of the MTC 1 unit (Figure 3a), which are characteristic features of MTC created by the dragging of coarser blocks within the MTC, and also indicate the flow direction (Posamentier, 2003). These grooves appear prominently in edge-detection attributes such as the Sobel filter attribute (Figure 3b). The relatively rare occurrence of these features indicates a relatively low energy of the initial flow, which contained a minimal amount of blocky material.

Attribute slices along the base of MTC 1 indicate a relatively continuous flow coming from the northeast. For instance, the horizon slice generated by blending coherent en-



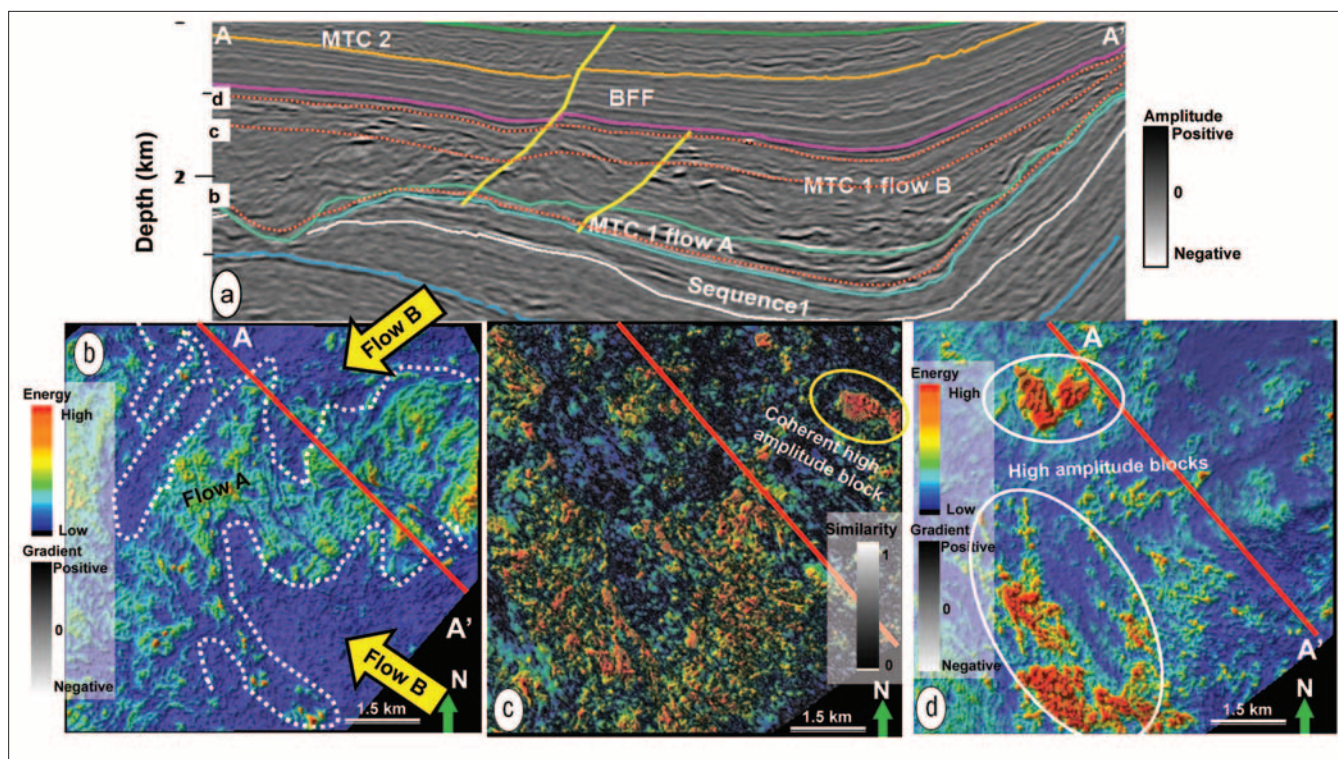


**Figure 4.** Stratal slices through MTC 1 sequence by corendering coherent energy and inline gradient volumes. Red dotted lines b, c, d in vertical seismic section in (a) represent stratal slices corresponding to the figures (b), (c), and (d) respectively. In (b) the white dotted line indicates encroachment of flow B into relatively continuous flow A from two directions. Stratal slice in (c) is also blended with low-coherent part of the energy ratio similarity attribute to identify coherent blocks and overall incoherent nature of flow B. (d) High-amplitude entrapped blocks toward the top of MTC 1 flow B.

ergy and inline amplitude gradient (Figure 4a) indicates the presence of a moderate to highly reflective coarser-grain matrix; however, this seismic geomorphologic pattern becomes chaotic upward through MTC 1 (Figure 4b). Extending this observation to the vertical seismic profiles, we subdivide MTC 1 into flows A and B (Figure 1c). Flow B is much more erosive in nature and gives rise to a chaotic seismic geomorphologic texture compared to flow A (Figure 4b). It encroaches into flow A from both the southeast and northeast (Figure 4a), eroding into underlying sequences in some places near the main conduit (Figure 1c). Within the overall incoherent pattern of flow B, some coherent high-amplitude blocks are entrapped as imaged in the stratal slice (Figure 4b) corendering coherent energy and amplitude gradient with the low-coherent part of the energy ratio similarity attribute.

Toward the top of MTC 1 flow B, we see relatively continuous stratification and some large entrapped high-amplitude blocks (Figure 4c). The strength and confined character of these bright spots suggest that they are hydrocarbon-charged sand bodies. If these bodies are sufficiently large, they can be exploited as a secondary exploration objective. More commonly, they are considered a potential drilling hazard to be avoided.

Although flows A and B are part of a large MTC unit, we interpret them as having completely different origins. Sandy debrites in flow A were generated due to basinal slope failure. These debrites entered into the salt minibasin as part of a fill and spill process, resulting in much reduced original force

and holding only a few coarser blocks. Consequently, flow A was much less erosive, shows a relatively less chaotic pattern, exhibits a broader flow conduit, and created very few striations or grooves at the base.

In contrast, flow B is extremely erosive and exhibits a highly chaotic seismic geomorphologic pattern. We interpret flow B of MTC 1 to have a local origin and to be formed due to collapse of sediment from in and around the minibasin in response to either salt diapirism or differential sediment loading.

**Basin floor fan unit overlying MTC 1.** Several stratal slices have been generated through the seismic sequence overlying MTC 1. We identify a basin floor fan within the seismic sequence in some stratal slices. A stratal slice (dotted line ii in Figure 5a) as shown in Figure 5c reveals the basin floor fan by plotting peak magnitude against peak frequency volumes. Distributaries and complex sediment distribution patterns within the fan are clearly seen on Figure 5e, which is a display of the coherent energy attribute blended with the inline coherent amplitude gradient attribute along this stratal slice. We abbreviate the sequence dominated by this basin floor fan as the BFF sequence. Two other stratal slices extracted at the top and bottom of the seismic sequence (5a) by blending peak magnitude with peak frequency exhibit monotonous, relatively low-amplitude pattern (5b and 5d). The feeder channels of the basin floor fan can be observed along a stratal slice at a shallower level (5a and 5f) to the main fan unit.

**MTC 2.** The basin floor fan sequence is overlain by MTC



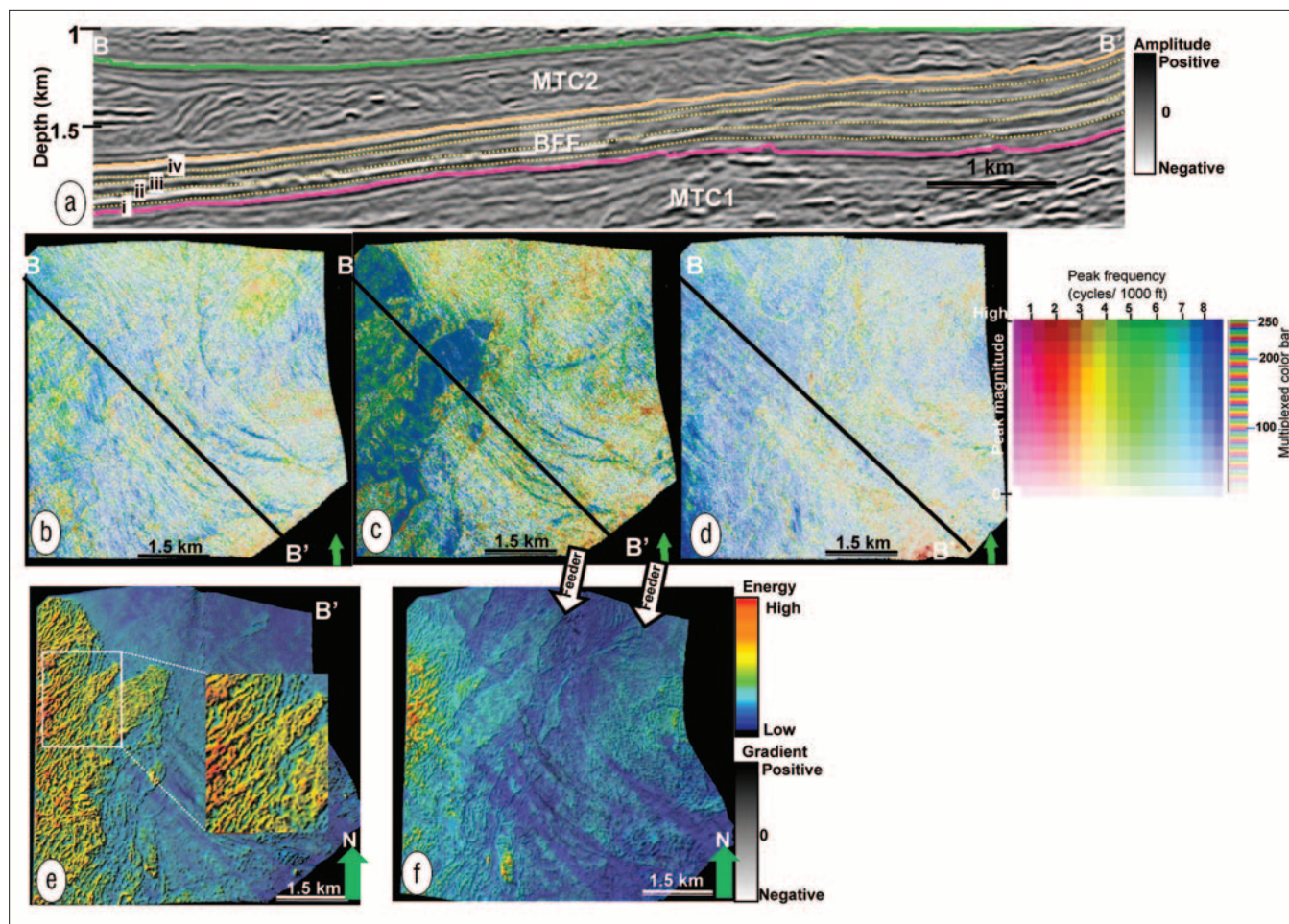


**Figure 5.** Stratal slices through basin floor fan (BFF) sequence. White dotted lines (i), (ii) and (iv) on vertical seismic profile in (a) correspond to stratal slices represented respectively in (b), (c), and (d) by blending peak magnitude with peak frequency volume against 2D hue-lightness color bar. Stratal slices (e) and (f) are generated by corendering coherent energy and inline gradient volume and they correspond to yellow dotted lines (ii) and (iii), respectively, in (a). Dotted line (ii) in (a) goes through the basin floor fan; whereas (i) and (iv) go through TST2 and TST3, respectively. Complex internal distributaries of the basin floor fan are illuminated in (e). (f) Reveals fan feeder channels.

2. The overall seismic geomorphologic pattern is chaotic in nature. MTC 2 does not have any erosional impact on the underlying and overlying units; consequently, it had significantly lower energy compared to flow B of MTC 1. MTC 2 contains some small slump blocks along with some debrites and undifferentiated MTC deposits (Figure 6a–6b). Overall analysis indicates that MTC 2 was related to basin-wide deposition rather than to salt tectonism. One of the most interesting features within MTC 2 is the presence of a higher-amplitude internal channel-submarine fan unit within the chaotic sediments as revealed by coherent energy and inline gradient blended stratal slice (Figure 6d). This channel appears as a high-amplitude strip within the MTC 2 unit in vertical seismic sections (6b). The chaotic sediments of MTC 2 are overlain by another blanket of low-amplitude sediments (Figure 6e).

**MTC 3.** MTC 3 is the uppermost sequence within the sedimentary column where the seismic data quality allowed geomorphologic analysis. MTC 3 does not yield any systematic depositional pattern from detailed seismic interpretation and seismic geomorphologic study. The overall chaotic facies

includes debris flows (Figure 6f) as well as combinations of slumps and debrites. Another low-amplitude interval is detected from seismic geomorphology at the top of this seismic sequence (Figure 6g).

### Sequence stratigraphic interpretation from sequential seismic geomorphologic patterns

Excellent vertical stacking patterns and well-defined seismic sequences created predominantly by the fill and spill processes are characteristic of salt minibasins (Winker, 1996). Sequential seismic geomorphologic analysis based on seismic attributes through these sequences provides a unique opportunity to estimate the relative sea-level changes and sequence stratigraphy of the minibasin as well as the whole basin. First, we attempted to define the sequence stratigraphic patterns from seismic geomorphologic studies alone. Then we made modifications in the relative sea-level curve by including the biostratigraphic information and finally compared the prediction with existing Quaternary eustatic cycles for the Gulf of Mexico (GOM).

Sequential seismic geomorphologic analysis as described

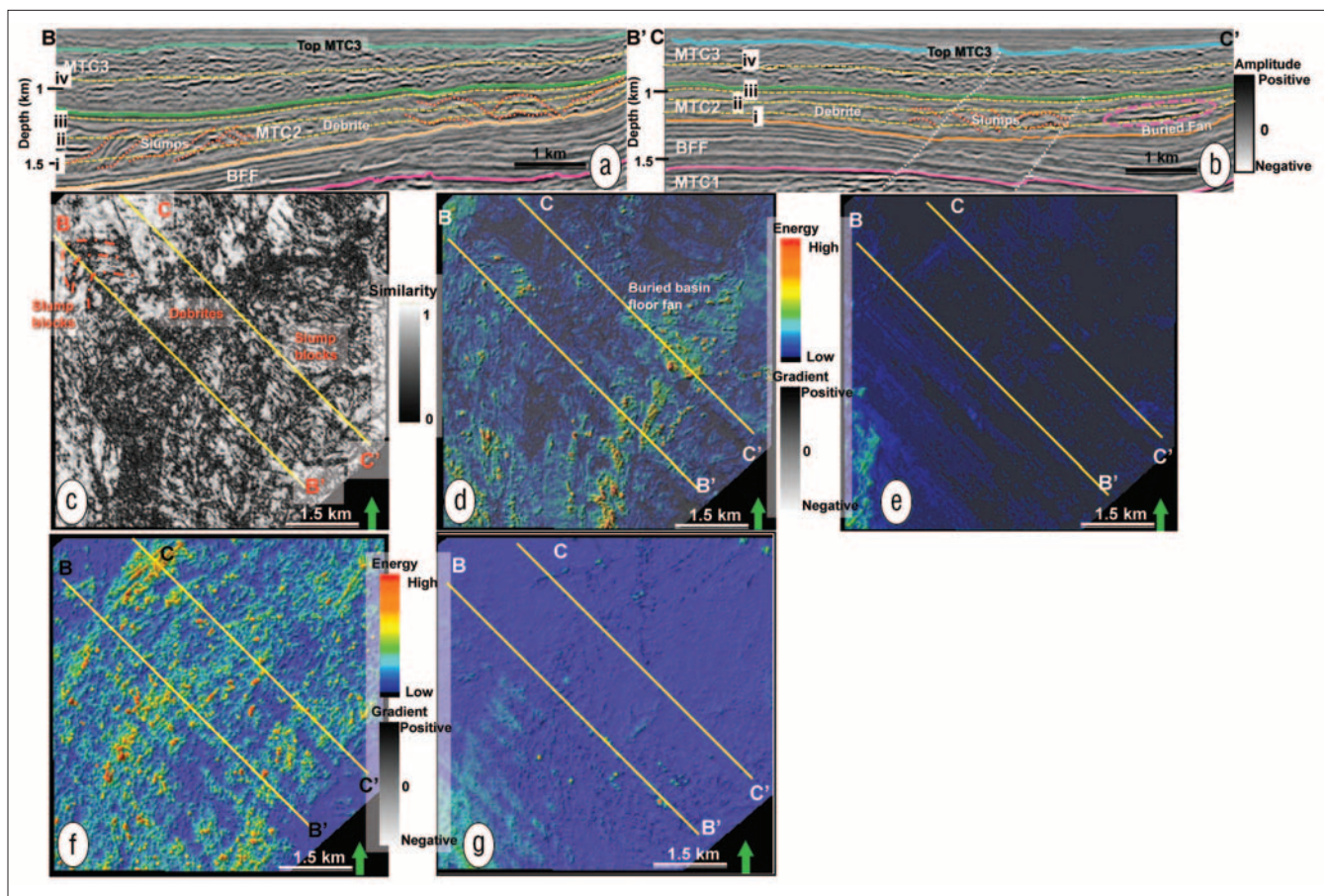


**Figure 6.** Stratal slices through MTC 2 and MTC 3 sequences. In vertical seismic lines (a) and (b), slumps and debrites are interpreted within MTC 2. Yellow dotted lines (i), (ii), (iii), (iv) in (a) and (b) correspond to stratal slices shown in (c), (d), (e), and (f), respectively. (c) Slump blocks, debrites, and overall chaotic nature within MTC 2 are imaged through the energy ratio similarity attribute. Stratal slices (d), (e), and (f) are generated by blending coherent energy with inline amplitude gradient attributes. (d) A buried basin floor fan within MTC 2 indicated by the pink ellipse in (b). (e) Monotonous low-amplitude deposits of TST 4 at the top of MTC 2. Sandy debris flow within MTC 3 is seen in (f). (g) Horizon slice at top MTC 3 horizon indicates initiation of low-amplitude blanket at TST 5.

Geologic time (Ma)	Calcareous nanoplankton	Planktonic foraminifera	Benthic foraminifera	Corresponding sequence top
.13		Globorotalia flexuosa		MTC3
.44	Pseudoemiliana lacunosa A			MTC2
.51		Globorotalia truncatulinoides		BFF
.64			Trimosina A	MTC1
.85	P. lacunosa variety			SEQUENCE1

**Table 1.** Last appearance datum of microfossils, their type and corresponding sequences in this study. (Biostratigraphic age data from Paleo Data, Inc., 2009.)

previously indicates that sequence 1 culminates with fine-grained sediments or shaly deposits which are in turn overlain by flow A of MTC 1. Since we interpreted flow A to be part of a basinal mass transport event, we hypothesize that the shaly deposit at the top of sequence 1 (Figure 2b) was formed during a transgressive systems tract (TST) and/or a highstand systems tract (HST). Sequence 1 was followed by flow A of MTC 1 (Figure 4b) in the early lowstand systems tract (LST) of the following sequence. We interpret base of MTC 1 flow A to be a sequence boundary. An increased sedimentation rate and differential loading caused enhanced salt diapir move-

ment throughout the basin, which resulted in the initiation of flow B above flow A within the same LST (Figure 4c). We interpret the monotonous relatively low-amplitude reflection pattern at the base of seismic sequence BFF to be finer clastics deposited during the next TST (TST 2) atop the MTC 1 unit (Figure 5b). Basin floor fans are formed during LST, such that the prominent basin floor fan in the sequence BFF was formed in the LST of the next sea-level cycle (Figures 5c and 5e). The feeder channel or canyon for this basin floor fan can be identified in the next shallower level (Figure 5f). Coarser sediments through the feeders were carried to the basin floor



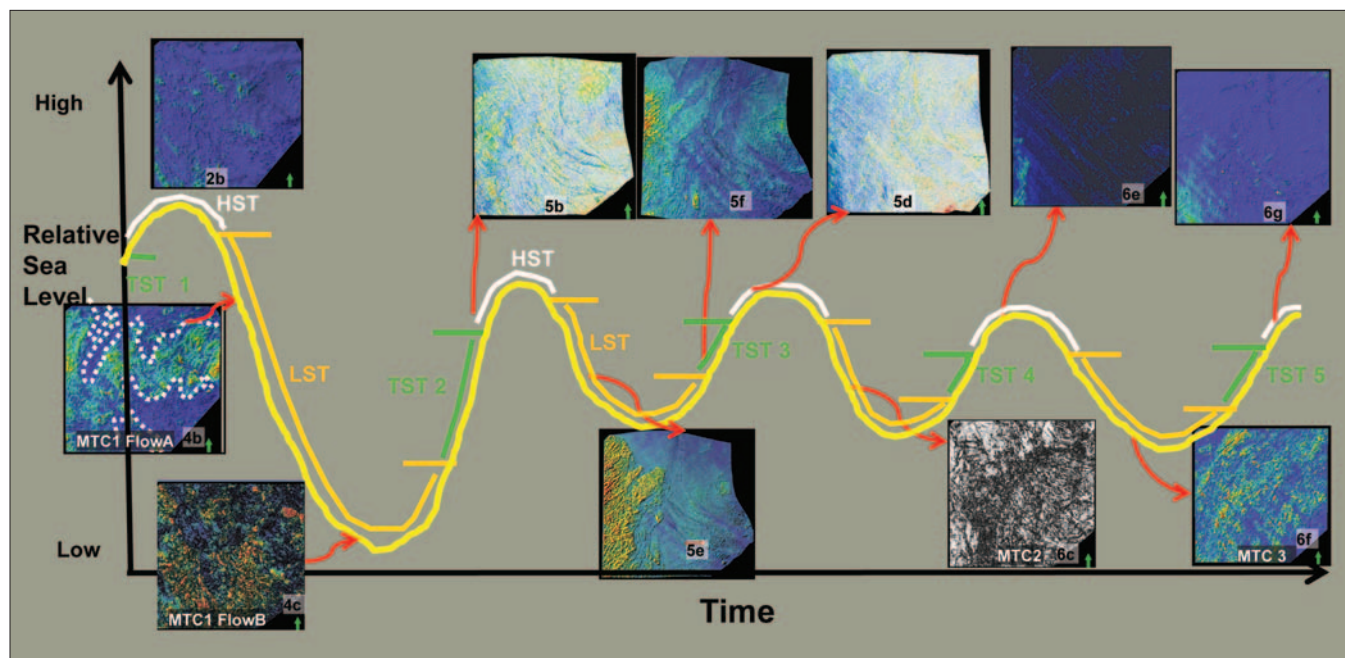


**Figure 7.** Generalized sea-level curve from sequential seismic geomorphology study. Orange, green, and white portions in each cycle represent LST, TST, and HST. The numbers associated with the images correspond to the original figure numbers.

fan, such that the channel conduits were open or filled with finer clastics. With the start of rising sea level during the TST (TST 3) following the LST, the depositional axes of the basin began to change such that the channels were backfilled

with coarser-grained material, making them visible through amplitude-sensitive seismic attributes. This TST 3 again deposited a blanket of finer clastics on the BFF sequence (Figure 5d). MTC 2 was a basinal event, formed during the next LST,

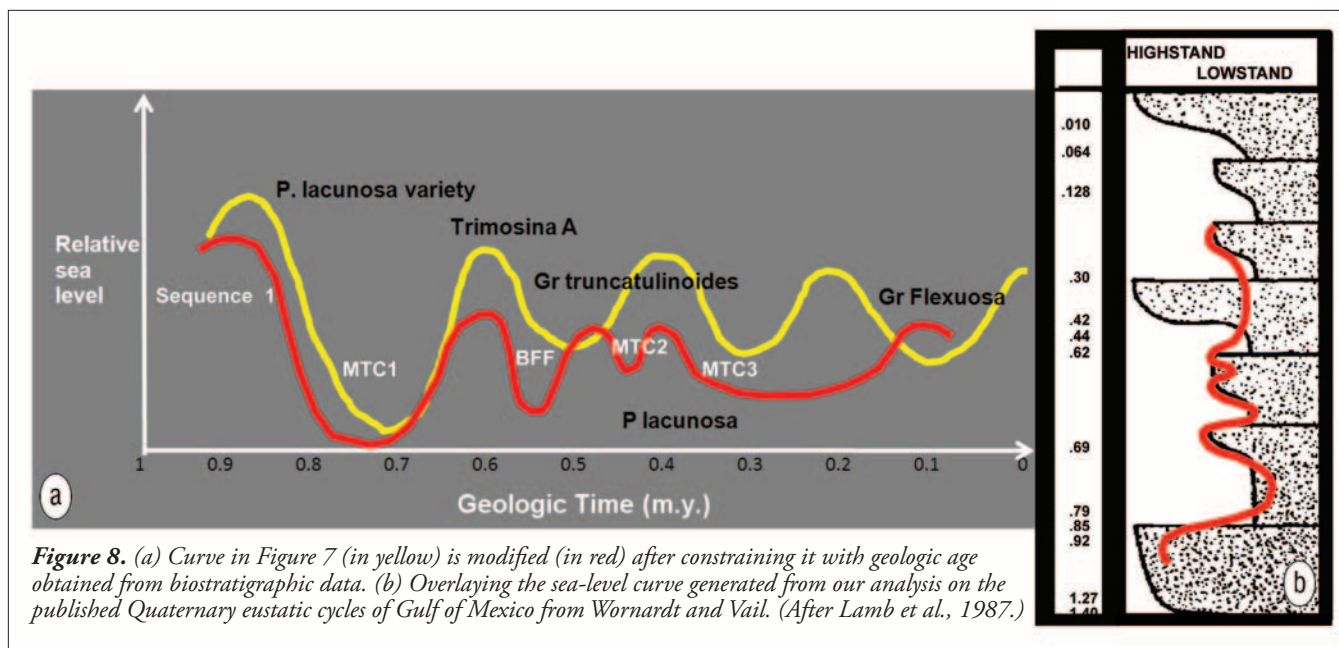


**Figure 8.** (a) Curve in Figure 7 (in yellow) is modified (in red) after constraining it with geologic age obtained from biostratigraphic data. (b) Overlaying the sea-level curve generated from our analysis on the published Quaternary eustatic cycles of Gulf of Mexico from Wornardt and Vail. (After Lamb et al., 1987.)

bringing some chaotic sediment into the minibasin. The buried channel-submarine fan unit was also formed during this LST and was buried within MTC 2. An additional blanket of low-amplitude sediments above MTC 2 is interpreted to be part of the next TST event (TST 4) (Figure 6e). We conclude our sequence stratigraphic analysis at MTC 3 (Figure 6f), which we interpret to be deposited during the next sea-level cycle, during a LST with finer clastics above it, indicating the beginning of a TST (TST 5) (Figure 6g). From this sequence stratigraphic interpretation based only on seismic geomorphology, we draw the preliminary relative sea-level curve shown in Figure 7.

The above sequence stratigraphic interpretation can be made during the early exploration stage, when only seismic data are available. In the following section we incorporate biostratigraphic information within our sequence stratigraphic framework for a more comprehensive picture before comparing our prediction with the available GOM eustatic cycles.

### Incorporating biostratigraphy within the seismic sequence stratigraphic interpretation

Biostratigraphy provides the ground truth for any sequence stratigraphic interpretation. Incorporating biostratigraphic information from the few wells in the area into the seismic sequence stratigraphic interpretation allowed us to make necessary calibration and changes to the existing curve (Figure 8a). We also verified whether we placed the MTCs in their proper sequence stratigraphic context. Table 1 shows the names of the key microfossils (corresponding to the sequences from the top of sequence 1 to the top of MTC 3), their type, and age of last appearance datum (LAD) as obtained from biostratigraphic chart for the Neogene section of the GOM. According to the biostratigraphic chart, these biomarkers represent either maximum flooding surfaces or sequence boundaries. Figure 8a shows the relative sea-level curve constrained by biostratigraphic age, showing that we

are examining fourth-order sequences ( $10^5$ – $10^6$  years).

### Comparison with existing eustatic cycles from the Neogene GOM

Finally we matched (Figure 8b) the newly constructed relative sea-level curve with the corresponding part of the Quaternary eustatic cycles from Wornardt and Vail (1991). The sea-level curve can be well correlated for the first two sequences, sequence 1 and MTC 1. BFF and MTC 2 correspond to a single sea-level cycle in the published curve, indicating that seismic data can sometimes lead to finer-scale information about sea-level change, especially within such shorter geologic time intervals. Denser biostratigraphic information is needed to understand its sequence stratigraphic significance. The next eustatic cycle does not match the newly constructed sea-level curve. Because the deposition of sediment within a minibasin predominantly follows the fill and spill pattern, sediments corresponding to this cycle might have bypassed, due to the lack of accommodation space left within the minibasin. The final part of the sea-level curve, corresponding to MTC 3 and planktonic foraminifera *Globorotalia flexuosa*, can be well-correlated with the eustatic cycle.

The relative sea-level curve we constructed from sequential seismic geomorphologic analysis corresponds reasonably well with the Neogene eustatic cycles. However, we observed that limited accommodation space within the minibasin may lead to some mismatch due to gaps in the sedimentary record. At the same time, some part of the sediment column may contain deposits resulting from local processes such as salt tectonics as happened in the case of flow B of MTC 1. Consequently, a one-to-one correspondence of the constructed sea-level curve for the sediments within the minibasin to the basin scale sea-level curve may not always be possible, although the points of mismatches may yield valuable information about missing or bypassed sequences.

## Summary and conclusions

Seismic geomorphologic features in the MTC-rich sediment column within a GOM minibasin were illuminated through seismic attributes. A bottom-to-top sequential geomorphology study of these features helped us to build a sequence stratigraphic framework.

We showed how to construct a relative sea-level curve from sequential seismic geomorphology and seismic sequence stratigraphic interpretation. This curve correlated well with the published eustatic cycles. In the absence of biostratigraphic data, the sequential seismic geomorphologic analysis from multi-attribute studies can provide a sequence stratigraphic framework for more detailed sand prediction. Combined with biostratigraphic information, such analysis may even reveal finer details not predicted by the regional sea-level curves. **TLE**

*Acknowledgments: We acknowledge Hess Inc. for the use of its deepwater GOM data volume for research and education and Schlumberger for providing the Petrel software, in which the interpretation was done. We acknowledge Belinda Ferrero-Hodgson, who did her MS thesis on these data and that was the starting point of our work. Much of the attribute software and financial support for the first author was funded by industry support for the Attribute-Assisted Seismic Processing and Interpretation consortium at Oklahoma University.*

*Corresponding author: supratik.sarkar@ou.edu*

## References

- Diegel, F. A., J. F. Karlo, D. C. Schuster, R. C. Shoup, and P. R. Tauvers, 1995, Cenozoic structural evolution and tectono-stratigraphic framework of the northern Gulf coast continental margin: AAPG Memoir **65**, 109–151.
- Ferrero-Hodgson, B., 2007, An integrated 3D seismic sequence-stratigraphic analysis of the Pleistocene strata above Baldpate Field, Garden Banks, Deep Water Gulf of Mexico: M.S. thesis, University of Oklahoma.
- Okuma, A. F., R. R. Pressler, D. B. Walker, and K. Kemp, 2000, Baldpate Field exploration history, Garden Banks 260, Gulf of Mexico: Gulf Coast Section-SEPM Foundation 20th Annual Bob F. Perkins Research Conference, 739–755.
- Paleo-data Inc., 2009, Biostratigraphic chart, Gulf Basin: USA-Neogene.
- Posamentier, H. W., 2003, Depositional elements associated with a basin floor channel-levee system: case study from the Gulf of Mexico: Marine and Petroleum Geology, **20**, 677–690.
- Winker, C. D., 1996, High-resolution seismic stratigraphy of a late Pleistocene submarine fan ponded by salt-withdrawal mini-basins on the Gulf of Mexico continental slope: Proceedings of the 28th Offshore Technology Conference, 619–628.
- Wornardt, W. W., and P. R. Vail, 1991, Revision of the Plio-Pleistocene cycles and their application to sequence stratigraphy and shelf and slope sediments in the Gulf of Mexico: GCAGS Transactions, **XLI**, 719–744.